On the computer simulation of a hydrophobic vitreous silica surface

V. A. Bakaev and W. A. Steele

Citation: The Journal of Chemical Physics **111**, 9803 (1999); doi: 10.1063/1.480317
View online: http://dx.doi.org/10.1063/1.480317
View Table of Contents: http://scitation.aip.org/content/aip/journal/jcp/111/21?ver=pdfcov
Published by the AIP Publishing

On the computer simulation of a hydrophobic vitreous silica surface

V. A. Bakaev and W. A. Steele
Department of Chemistry, 152 Davey Laboratory, Penn State University, University Park, Pennsylvania 16802

(Received 11 August 1998; accepted 8 September 1999)

The experimental evidence that the surface of pure vitreous silica can be hydrophobic imposes strong limitations on possible atomic configurations at that surface. This is due primarily to the fact that the electric field of the partially ionic SiO_2 can have very strong interactions with adsorbed polar molecules and with water in particular. The simulations reported here indicate that a surface structure consisting of a random net of almost regular corner-sharing SiO_4 tetrahedra with a low concentration of defects such as nonbridging oxygen atoms is capable of producing hydrophobicity. It is shown that the defects as well as distortion of the SiO_4 tetrahedra as measured by their dipole and quadrupole moments give rise to hydrophilic adsorption sites on the surface. Computer simulation of such a random net at a surface runs into a general problem typical of computer simulations of amorphous solids: at temperatures near to but above the glass transition temperature, the time scale of the molecular dynamics is many orders of magnitude less than the experimental structural relaxation times of the material. A solution to this problem was obtained here by imposing a constraint on the molecular dynamics simulation that directs the chain of simulated configurations toward one without nonbridging oxygens. This is demonstrated by showing that the binding energies of a water molecule over the surface of this solid are smaller than the energy liquefaction, which is taken here as the criterion for hydrophobicity. © *1999 American Institute of Physics.* [S0021-9606(99)70345-4]

I. INTRODUCTION

Surface chemical and physical properties are fundamental to an understanding of observables such as strength, corrosion, polymer adhesion, and bioreactivity of glasses as well as the properties of electronic devices using silica and optical fibers. The surface structure is the basis for understanding of those properties on an atomic level. Computer simulations of the vitreous silica surface could play important role in elucidating its atomic structure.

However, despite the abundance of computer simulations of bulk silica and silicate glasses and melts,[1] the computer simulations of their surfaces seem to be limited to those reported by Garofalini and co-workers (see Refs. 2–7 and references therein). The basic conclusion is that there is a considerable concentration of topological and bonding defects in vitreous silica surfaces.[4] Among these defects, nonbridging oxygen atoms (NBOs) are present in the largest concentration (1.9 per 100 $Å^2$). The validity of this result was confirmed by the fact that the estimated concentration of OH groups (6.4/100 $Å^2$) on the hydroxylated material agreed favorably with experimentally determined values (4.5–6.2 per 100 $Å^2$). Since the simulated surface did not contain OH groups, this estimate was made by associating one OH group with each NBO, two OH groups to every two- and three-membered ring etc.

There is no direct experimental evidence that NBO (dangling bonds) really exist at the surface of vitreous silica. Experiments rather testify to the contrary: The early ESR experiments did not detect radicals corresponding to NBO on a freshly fractured silica surface.[8] It was assumed that the most probable explanation for this fact was the reconstruction of the surface that eliminates dangling bonds and NBOs. This point of view was confirmed by XPS measurement as reviewed in Ref. 9 and the conclusion was that there are no measurable NBOs on the surface of freshly fractured vitreous silica. The XPS spectrum of the O 1*s* photoelectrons from the surface of pure fused silica fractured in ultra high vacuum consisted of only one line corresponding to bridging oxygen.[10] Thus XPS as well as ESR suggest an absence of NBO at the freshly fractured surface of vitreous silica and we do not know any other experiment that shows NBOs at that surface.

However, this experimental evidence is not conclusive: One might argue that a NBO does not necessarily produce a paramagnetic radical detectable by ESR. The XPS result also can be inconclusive since the penetration depth of O 1*s* photoelectrons is on the order of a few nm whereas the NBOs are expected in a surface layer a fraction of nm thick and thus might not influence the XPS spectra.[11] (However, XPS does detect O 1*s* signal from surface OH groups.[10])

The present study is devoted to an attempt to simulate the hydrophobic surface of vitreous silica. Silica and silicate surfaces are generally classified as hydrophilic and hydrophobic according to their affinity toward water. According to one criterion, hydrophilic surfaces are those which bind water molecules with energy greater than the heat of liquefaction, 44 kJ/mol, and hydrophobic surfaces are those that bind water molecules with energy smaller than this heat.[12] This definition was used in conjunction with simulations employing a conventional molecular dynamics algorithm to show that nonhydroxylated hydrophilic silica surfaces can be gen-

erated relatively easily and that many of the structural properties of such surfaces are qualitatively quite similar to those obtained in the previous simulations. However, most of the effort in this study is devoted to an attempt to simulate the hydrophobic surface of vitreous silica. The reason for that is that we expect a quasiequilibrium (as close to thermodynamic equilibrium as an amorphous surface can be) surface of dehydroxylated vitreous silica to be hydrophobic.

In a general review of the properties of water on silica, it was argued the the hydrophobic sites on its surface are siloxane bridges (Si–O–Si) and well separated (free) silanol (SiOH) groups[12] and the hydrophilic sites are primarily due to vicinal silanols. A silica surface containing pairs of vicinal silanol groups will be hydrophilic, but at temperatures of 500–1000 °C, two neighboring OH-groups will condense into a water molecule and evaporate, converting the vicinal silanol groups into a siloxane bridge. The resulting silica surface contains only isolated silanols and siloxane bridging oxygens and is hydrophobic. These facts are well known and reviewed in more detail in Ref. 13. Thus, the hydrophobicity of the fully dehydroxylated silica surface can be ascribed to the poor affinity of water for the siloxane bridges (see, e.g., Ref. 14 and references therein). Supporting evidence is given by studies of the internal surface of a pure crystalline porous silica ZSM-5 (silicalite) which consists only of siloxane bridges and is ''unusually hydrophobic.''[15] Also the surfaces of mesoporous silica crystals or pyrogenic silica which do not contain OH-groups because they are produced without contact with water are hydrophobic.[16] Based on this experimental evidence, a simulated surface of amorphous silica that contains no silanol groups at all should be hydrophobic.

The atomic structure of bulk amorphous silica is usually considered as a random network of corner-sharing regular tetrahedra.[17,18] An ideal random network does not contain topological defects like NBOs or edge-sharing tetrahedra and the SiO_4 tetrahedra are near perfect as in crystalline polymorphs of silica.[17] However, in amorphous silica, especially at a surface, the tetrahedra might be distorted and, in addition, NBOs might be expected to be present. As shown in Sec. IV, these defects induce strong electrostatic interactions with water molecules and thus give rise to hydrophilic adsorption sites on non-hydroxylated silica surfaces. Thus, if one is to simulate the hydrophobic silica surface, it is necessary to exclude atomic configurations with high concentrations of distorted tetrahedra and NBOs. At this point, we introduce the term ''defect oxygen'' (DO) to avoid confusion with the term NBO used for a single coordinated oxygen. Here, a DO means an oxygen atom with any coordination with respect to silicon atom except 2. The reason for this notation is that in Sec. IV we show that DOs are associated with hydrophilic sites and thus, their elimination in the simulation is necessary to obtain the desired hydrophobic surface.

It has been shown that a bulk amorphous silica atomic configuration with a very low concentration of DOs and very small distortion of tetrahedra can be simulated with the TTAM interatomic potential by a very slow (on molecular dynamics time scale) annealing that starts from a liquid configuration at 4000 K.[19] The TTAM potential is convenient for simulations particularly because it is a two-body function, and thus it is the one chosen for this study.

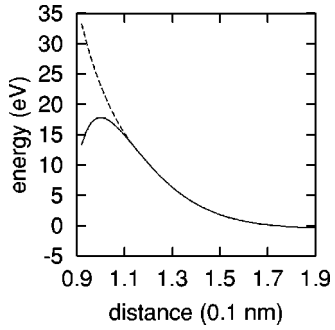

FIG. 1. Modified repulsive part of TTAM potential for O/Si interaction. Solid line: original TTAM Eq. (1). Dashed line: modified TTAM Eqs. (1) and (3).

The next section considers interatomic potentials and especially those for the water/silica interaction. We consider here only physical adsorption of water (the chemisorption was simulated in Refs. 20 and 21).

II. INTERATOMIC POTENTIALS

The interatomic potentials used in this paper for the simulation of bulk silica and the silica surface describe the interactions between the ions in silica as well describing interaction of that surface with a water molecule. The interactions in silica are described by the TTAM potential[22] consisting of the Coulomb interaction of point charges of +2.4 and -1.2 placed on the Si- and O-positions, respectively (here and below the unit of charge is the electron charge) and van der Waals (vdW) type interactions between those particles. The vdW part of TTAM is written as

$$u_{ij}(r)=f_0 h_{ij}\exp\left(\frac{R_{ij}-r}{h_{ij}}\right)-\frac{c_{ij}}{r^6} \tag{1}$$

with a combination rule

$$R_{ij}=R_i+R_j,\ h_{ij}=h_i+h_j,\ c_{ij}=c_i c_j \tag{2}$$

where R_i, h_i, and c_i are parameters ascribed to an individual i-atom. Thus this component of the TTAM has a Born–Mayer repulsive term with the Gilbert parametrization[23] and an attractive term that plays the role of the dispersion energy. The Gilbert parametrization introduces a standard force f_0 that is used to determine the scale of ionic radii: like distance between two ions (i and j) squeezed by the standard force depends upon their radii R_i and R_j and the softness parameters h_i and h_j. These parameters as well as the dispersion interaction type parameter c_i and effective electrical charges for Si and O atoms were obtained by fitting the energy surfaces of a SiO_4^{4-} cluster in a crystalline field. The energy surfaces were obtained from *ab initio* Hartree–Fock SCF calculations. Such *ab initio* potential models are now considered to be the most accurate for silica (see, e.g., Refs. 24–26 and references therein).

A minor technical problem with Eq. (1) is that at very small separations it has a maximum (cf. Fig. 1). This unphysical behavior of TTAM at small distances may influence the computer simulation at very high temperatures so that in

those cases it is usually slightly modified.[25] In this paper TTAM was also modified in the following way: For two ions of *i*- and *j*-types the value of the maximum energy for Eq. (1) was determined and at the larger of two distances r_0 that correspond to 0.7 of that energy the potential of Eq. (1) was set equal to the repulsive term

$$u(r)=B/r^n \tag{3}$$

so that the values of $u(r_0)$ and their derivatives coincide for Eqs. (1) and (3). The modified vdW part of TTAM that coincides with Eq. (1) at $r>r_0$ and with Eq. (3) at $r<r_0$ is shown in Fig. 1 for O/Si interaction with $r_0=1.15$ Å. (For O/O, $r_0=1.81$ Å, $u(r_0)=4.1$ eV and for Si/Si, $r_0=0.12$ Å, $u(r_0)=10^8$ eV.)

For the interaction of a water molecule with the silica surface, we will start from one of the best (empirical) water–water potentials and use combining rules to obtain the various pairwise potentials that make up the water/silica interaction. The TIP3P, TIP4P, and SPC are regarded as the best available models of water today but they are usually found to be brittle.[27] This means that they are highly optimized to reproduce the bulk properties of water and may fail when extended to other systems, e.g., description of clay/water or silica/water interaction. Recently more robust water/water potentials were tested in bulk water simulations.[27] These have the same structure as TTAM and TIP or SPC models, again consisting of vdW and Coulomb parts. It has been found that the best results are given by a model that combines the point charges of TIP models with a vdW part from a more robust potential; the model that used point charges obtained from semiempirical SCF yielded unsatisfactory results.[27] Thus the water/water interaction adopted in this work is based on the SPC model[28] that is as good as TIP3P and TIP4P in simulations of liquid water but a little simpler. It places -0.82 and $+0.41$ point charges on O- and H-positions in a water molecule and a Lennard-Jones force site on the O-position:

$$u_{ij}(r)=4\epsilon_{ij}\left[\left(\frac{\sigma_{ij}}{r}\right)^{12}-\left(\frac{\sigma_{ij}}{r}\right)^{6}\right] \tag{4}$$

with $\epsilon_{11}=0.650$ kJ/mol, $\sigma_{11}=0.316$ nm as parameters. [Here indexes are not necessary; they are preserved for comparison of Eq. (4) with Eq. (1).] The geometry of the model is determined by tetrahedral H–O–H angle and 1.00 Å for OH distance.

To obtain the potential of interaction between a water molecule and the atoms of silica, TTAM and SPC were combined. The effective charges on Si, O in silica and H, O in water were the same as prescribed by TTAM and SPC. The LJ part of SPC was converted into the TTAM form by a requirement for Eq. (1) to have the same minimum energy separation (r_{ij}) depth (ϵ_{ij}) and the same behavior for $r\rightarrow\infty$ as Eq. (4). This holds when

$$h_{ij}=r_{ij}/12;\ R_{ij}=r_{ij}\left[1+\frac{1}{12}\ln\left(\frac{12\epsilon_{ij}}{f_0 r_{ij}}\right)\right];$$
$$c_{ij}=4\epsilon_{ij}\sigma_{ij}^6;\ \ r_{ij}=(2)^{1/6}\sigma_{ij}. \tag{5}$$

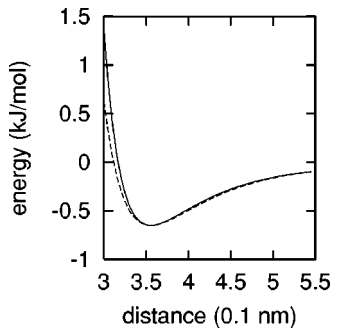

FIG. 2. Lennard-Jones part of the SPC potential for O/O interaction of water converted to the TTAM form. Solid line: LJ potential Eq. (4). Dashed line: TTAM Eq. (1) with parameters from Eq. (5).

This equation ascribes the parameters R_i and h_i to the O-atom of a water molecule so that now one can calculate the vdW part of the SPC model by Eq. (1). A comparison of the two forms is presented in Fig. 2.

Formally the transformation of the vdW part of SPC to the TTAM form through Eq. (5) makes it possible to calculate the interaction of a water molecule with O- and Si-ions of silica (and potentially with other ions of multicomponent glasses for which Gilbert parameters are known). The purpose of such a transformation is to make SPC a more robust interatomic potential (in the sense of Ref. 27). The hope that this might be the case is based on the fact that the Gilbert parametrization has some theoretical justification and physical appeal in contrast to totally empirical SPC (or TIP) models. However, Eq. (2) includes a combination rule for c_{ij} that is not part of the Gilbert parametrization but a separate combination rule for dispersion energy constants. The problem with this combination rule is that although the c_i coefficient for the SPC model from Eqs. (4) and (5) might really represent the dispersion interaction of two water molecules, the similar coefficients in Eqs. (1) or (2) are just lumped parameters. Normally one would expect the dispersion interaction of two oxide ions to be of the order of magnitude of that for two Ne atoms isoelectronic with O^{2-} ions. For Ne, the values of ϵ and σ in Eq. (4)[29] give the dispersion energy constant [c_{ij} in Eq. (5)] 4.7 times less than that for O/O interaction in SPC but about 150 times less than c_{ij} in Eq. (1) for O/O interaction in TTAM. Therefore it is not reasonable to use the c_i coefficients for the O-atom in TTAM to calculate the water/silica interaction. Instead the SPC c_{11} coefficient from Eqs. (4) and (5) was used and $c_{12}\approx 0$ (in c_{ij}, $i=1$ for O and $j=2$ for Si).

All the interatomic potentials used here are pairwise so that to calculate an energy or a force acting on an atom it is necessary only to add up the inputs from separate atoms. The summation of electrostatic contributions was performed by Ewald's method. For the simulation of the bulk silica, 1661 vectors of reciprocal lattice were included in the summation. For the simulation of a surface layer that has periodicity only in the *X*- and *Y*-directions, the same method with periodicity in the *X*-, *Y*-, and *Z*-directions was used but the period along the Z-direction was taken to be twice as large as in the *X*- and *Y*-directions. This increased the number of the reciprocal lattice vectors included in the summation to 2365. The ficti-

tious periodicity along the *Z*-direction implies the presence of copies of the original surface layer above and below the original but their electrostatic interaction with the original layer is assumed to be small since the electrostatic field decreases very rapidly with the distance between layers.

III. COMPUTER SIMULATION

Sixty years of diffraction studies of vitreous silica have confirmed the validity of the random network model of its atomic structure.[18] The data show that the tetrahedra in the random network are almost regular with O–Si–O angles close to the tetrahedral angle (109.7 ± 0.4) and Si–O and O–O distances around 1.61 Å and 2.63 Å, respectively. However the Si–O–Si angles are broadly distributed around 140–150 degrees which is the main structural distinction between amorphous silica and its crystalline polymorphs.[18] The detailed comparison of MD computer simulation using three-body interatomic potentials with the results of diffraction studies showed a reasonably low (9.1%) reliability factor (for comparison, the reliability factor obtained using reverse Monte Carlo techniques is 2%) but SiO_4 tetrahedra are still too distorted relative to experiment.[18]

It seems that somewhat better results for the bulk were obtained in a MD computer simulation using TTAM[19] than with the three-body potential. Although in Ref. 19 there was no detailed comparison of simulated and experimental radial correlation function and the TTAM Si–O distance was a bit larger than experimental, the tetrahedra were almost regular (judging by the narrow O–Si–O angle distributions) and the level of coordination defects was 0.4%. [The concentration of coordination defects in Ref. 19 is evaluated here as the ratio of all the atoms whose coordination is different from that typical for the random net model (4 for Si and 2 for O) to the total number of atoms—see below.] Thus the atomic configuration simulated in Ref. 19 was very close to the ideal random net of corner-sharing regular tetrahedra. This was achieved mainly by annealing the initial random configuration of atoms from 4000 K to 1400 K with a cooling rate 2.5×10^{13} K/s. This is an exceedingly fast cooling rate in comparison to those occurring in nature but by molecular dynamics standards it is very slow since the cooling took 10^5 time steps of 1 fs each. With such a rapid cooling rate one should not expect to reproduce all the peculiarities of liquid silica behavior in the region of the glass transition.[19] In general, rapid cooling rates are a major problem with the MD simulation of glasses so that the simulated structures can be appropriate to much higher fictive temperatures.[18] Nevertheless, in this work, we essentially followed Ref. 19 (that is, used simple annealing) in the first stage of the simulation since our main objective at this stage was just to simulate a good random net structure of bulk amorphous silica. Thus 360 atoms of SiO_2 were placed in a cubic simulation box. This number of atoms is about two times less than that used in Refs. 4 and 19 but is slightly larger than the smallest system in a recent work on size effects in the computer simulation of liquid silica[30] where it was shown that static structural quantities, such as the RDF or the partial structure factors for their smallest system (336 atoms) do not differ from those with 1002 or even 3006 atoms. Although there may be some small size effect on the surface properties, the small system was chosen in order to perform extensive annealing studies (see below) with workable computing times.

Initially, the 360 atoms were distributed quasi-randomly in a box of edge length 20 Å (quasi-randomly because configurations with strongly repulsive overlapping particles were excluded). This system was equilibrated using a standard NPT-ensemble Monte Carlo (MC) algorithm[31,32] with three-dimensional periodic boundary conditions (PBC) at a temperature of 3000 K and a pressure of 1 bar. As the number of Monte Carlo trials increased, the control charts of energy and density showed equilibration to values that fluctuated around constants. The equilibrium edge length of 17.6 Å corresponded to the desired density of 2.2 g/cm^3. At this point, the simulation was changed to constant energy MD using the velocity Verlet algorithm with a time step of 2 fs. (For this time step, the standard deviation of the total energy from the required constant value is about 0.01%). In this way, annealing was performed for 40 ps at ca. 2100 K and then for 16 ps more at ca. 950 K. At this point, the concentration of DOs in the bulk silica atomic structure was 0.8%. This concentration is obtained here by determining the four nearest O-atoms to each Si-atom and calling this a tetrahedron. This group is unique for each Si-atom but may differ considerably from a regular geometrical tetrahedron. If an O-atom belongs to two tetrahedra, it is a normal bridging oxygen. All other oxygen atoms are considered to be DOs according to the definition in Sec. I. These include free oxygens that do not belong to any tetrahedron (coordination 0), DOs with coordination 1, and all the DOs with coordination more than 2. Since the coordination of Si-atoms with respect to O-atoms is 4 by definition, they are excluded from consideration of topological disorder in this scheme. This description of the coordination of ions in silica differs from that usually adopted in the literature where Si- and O-atoms in the bulk are considered bonded when their distance is less than some prescribed value [e.g., 2 Å, Ref. 4]. This definition is justified by the fact that the radial distribution function (RDF) in simulated vitreous silica has a sharp peak at a distance of about 1.6 Å and is almost zero between 2 and 2.5 Å (see, e.g., Fig. 1 in Ref. 19). Note that the area of this sharp peak is 4.000 (see Table I in Ref. 19) which means that each Si-atom has almost always 4 nearest O-atoms. To the extent that these results are applicable to the surface layer of SiO_2, they indicate that the evaluation of the positions of the four nearest neighbors to each Si is a reasonable way to characterize its nearest neighbor environment. As will be shown below, this representation of the nearest neighbor distribution is quite convenient when it comes to the calculation of the electrostatic field at the surface (or the minimum surface–water interaction energy) which is so important in determining hydrophobicity. We emphasize that this new definition, in fact, does not contradict the usual one: if one finds a strongly distorted tetrahedron of O atoms around a Si atom, one can always find an O atom with a large distance from Si (say, more than 2 Å) and declare the Si atom undercoordinated.

Another reason to adopt the definition given here is the following. The state of a Si atom in silicates can be detected

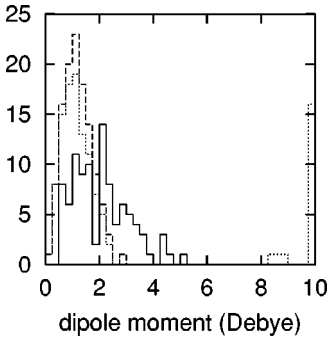

FIG. 3. Distributions of dipole moments of SiO_4 tetrahedra in the simulated atomic configurations. Dashed line: initial bulk configuration. Dotted line: initial surface configuration. Solid line: final surface configuration.

by NMR (see, e.g., the review in Ref. 33). The NMR spectra sometimes display weak bands with unusually large chemical shifts which are interpreted as five- and six-coordinated Si atoms (see, e.g., Fig. 5 in 33). However, what NMR really sees is not the coordination of a Si atom but a distortion of electron wave function around ^{29}Si nucleus. The latter certainly can be interpreted as the consequence of a change of coordination but it is also appropriate to say that the electron wave function around ^{29}Si nucleus is distorted (has lower symmetry) because the oxygen tetrahedron centered around that nucleus is distorted.

After the bulk silica atomic structure was obtained by the above method, the PBC in the *Z*-direction was removed and 48 O-atoms and 24-Si atoms at the bottom of simulation box were fixed. In this way, the remaining 288 atoms made up the surface layer and thus were taken to be mobile in the MD simulation. This is essentially the procedure of Ref. 4. As a result of PBC removal, the concentration of DOs jumped from 0.8% to 9.9%. More specifically, the initial surface configuration contained 173 bridging oxygens and 19 DOs among which 11 single and 8 triple coordinated oxygens were observed. (Only O-atoms in the mobile surface layer are considered; otherwise the number of O-atoms with single and triple coordination would be equal.) This jump of the concentration of DOs occurs because some tetrahedra at the surface are destroyed upon removal of PBC. According to the description that is being used here, the Si-atoms of those tetrahedra will still preserve their fourfold coordination, but these tetrahedra are now strongly distorted. This can be seen from the calculations of the distribution of the dipole moments of tetrahedra that is shown in Fig. 3. To calculate the dipole moment of a tetrahedron, the electric charge of an O-atom (the TTAM value) was divided by its coordination number since only that fraction of the atomic charge belongs to each of the tetrahedra. Letting this charge be q_m and the vector between the charge and the central Si be $\mathbf{r}_m$, the dipole moment of the group of five ions will be $\Sigma_{m=1}^{4} q_m \mathbf{r}_m$. The dashed histogram in Fig. 3 shows the distribution of dipole moments in bulk silica simulated as described above. It is a relatively narrow distribution that testifies to the low distortion of the tetrahedra in the bulk. Upon removal of the PBC, this histogram splits into two peaks (dotted plot): one below the dashed histogram and another on the right side of Fig. 3. The latter is due to highly distorted surface tetrahedra whose dipole moments are equal or larger than 8 Debye. As will be shown in the next section, these distorted surface tetrahedra produce strongly hydrophilic sites on the surface. Thus the main problem in this work was to find a method of annealing this surface configuration to eliminate them.

Since the dipole (and the quadrupole) moments of regular tetrahedra are zero by symmetry, the distributions of dipole (and/or quadrupole) moments is a convenient measure of their distortions from perfect tetrahedral symmetry. Furthermore, the dipole moments of the tetrahedra in the surface layer of silica can be used to calculate the surface electrostatic field or, more importantly, the electrostatic energy of a water molecule located near the silica surface. The method used to determine the field of minimum energies (negative binding energies) of a water molecule over the silica surface was to evaluate the energy of interaction of a water molecule by summing the Coulombic and the dispersion/repulsion energies over the atoms in the water molecule with all the Si- and O-atoms, as described in Sec. II. In this way, one obtains the potential energy of a water molecule at any point (x,y,z) above the silica surface for any orientation of the water as determined by its three Euler angles (θ, φ, ψ). The field of minimal energies is $U_{\min}(x,y)$ which is the value of $U(x,y,z,\theta,\varphi,\psi)$ minimized with respect to θ, φ, ψ, and z. This minimization was carried out basically by the conjugated gradient method.[34] However, the conjugated gradient minimization sometimes drove the molecule far from the surface where a second (very shallow) minimum of U is situated. To overcome this problem, preliminary MC minimization was performed that decreased U to some small positive value.

The results obtained for water over the initial SiO_2 surface suggest that the annealing of the initial surface requires considerable structural rearrangement in the surface layer to obtain the desired surface. The preliminary annealing toward a hydrophobic surface carried out here was based on the following algorithm: At each time step of the MD the velocities were rescaled so that the kinetic energy of the mobile atoms exactly corresponded to the temperature:

$$T(t) = T_{\max} + (T_{\min} - T_{\max})[1 - \exp(-t/\tau)]. \tag{6}$$

This time profile of temperature was chosen because the structural rearrangement requires progressively more time in final stages of temperature annealing than in the initial ones but this method of velocity rescaling does not exactly model a real temperature annealing. A refinement of the method, (e.g, as in Ref. 19) is possible but is not justified here since it seems that one can not model real temperature annealing of glass anyway due to computer time limitations.

The minimum potential energies of a water molecule $U_{\min}(x,y)$ on a vitreous silica surface obtained from the initial surface by simple annealing with temperature exponentially decreasing from 4000 K to 270 K for 20 ps [Eq. (6) with $T_{\max}=4000$ K, $T_{\min}=270$ K, $\tau=2$ ps] is shown in Fig. 4(a). Although the number of DOs decreases initially during the annealing, it was found that after 4 ps when the temperature had reached 775 K, the number of these defects fluctuated around a constant value of 7 ± 1 % per 192 Os. After 20

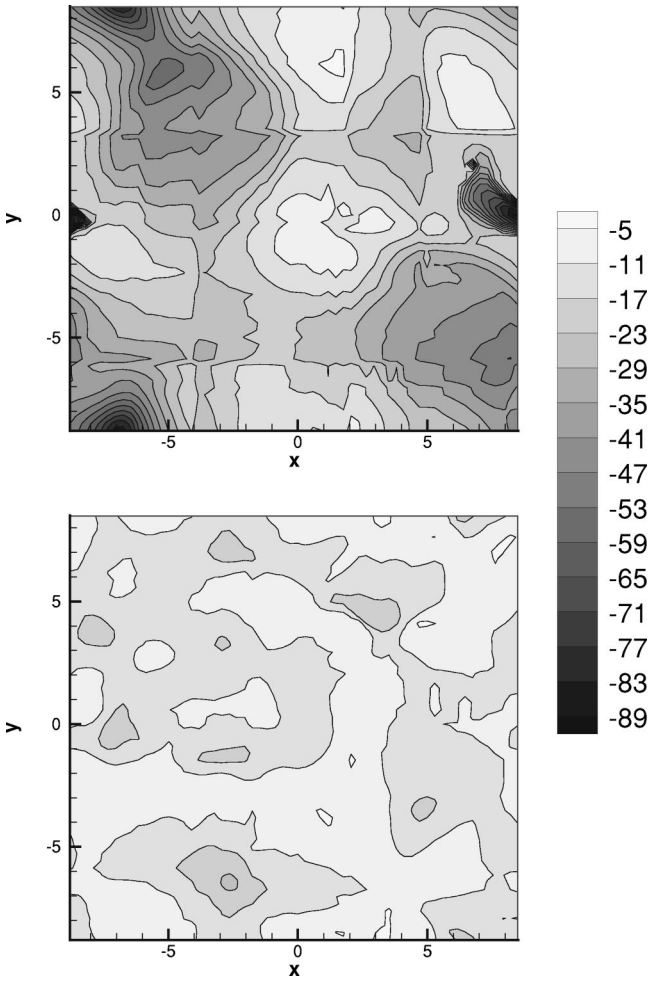

FIG. 4. Distribution of minimal energies of a water molecule on a vitreous silica surface. Energies in kJ/mol are shown on a scale to the right of pictures; distances on axes are in Å. The surface layer of upper picture (a) contained 178 bridging oxygens and 14 DOs (7 single and 7 triple coordinated O-atoms). The surface layer of the lower picture (b) contained 192 bridging oxygens and no DO.

ps, the surface atomic configuration of Fig. 4(a) was obtained that contained 7 singly, 178 doubley, and 7 triply coordinated oxygen atoms per 309 $Å^2$ in a surface layer 13.2 Å thick. This may be compared to the concentration of DOs in vitreous silica surfaces as reported in Ref. 4: 1.9 singly coordinated oxygens per 100 $Å^2$ of the 1.1 Å thick outer layer of the surface and 1.4 triply coordinated oxygens per 100 $Å^2$ located 3–5 Å into the surface. It is clear that the level of topological disorder at the surface in Fig. 4(a) is about the same (or smaller, if referred to the 1 Å thick surface layer) than that reported in Ref. 4.

The minimum potential energy surface for water interacting with the partially annealed SiO_2 that is shown in Fig. 4(a) indicates that there are several adsorption sites on the surface where the minimum potential energy of a water molecule is more negative than the negative of heat of liquefaction of water at room temperature (−44 kJ/mol). Thus, this simulation has not produced a hydrophobic surface. After many unsuccessful attempts to eliminate DOs in the initial surface layer by modeling the temperature annealing with the help of MC as well as MD computer simulations, the following method proved to be successful: Starting from a surface layer with an atomic configuration obtained by removing the PBC, a MD simulation was begun using temperature-time profile determined by Eq. (6). At each time-step the number of DOs was determined. If the number of DOs did not increase from the number present during the previous time step, the step was accepted and the next step performed as usual. If the number of DOs increased, the step was rejected, the velocities of all the particles were discarded and the new velocities were chosen at random from the Maxwell distribution corresponding to the current temperature. This method of annealing introduces some elements of MC-like rejection of some trial configurations in the MD simulation. However, this is done not to simulate some real process but to direct the chain of MD configurations toward a configuration without DOs. Once this configuration is reached, all acceptable succeeding configurations do not contain DOs and one can simulate the development of symmetrical tetrahedral environments in the system.

The minimum potential energy surface for a water molecule over a surface generated in a typical annealing simulation of this kind are shown in Fig. 4(b). The surface layer of the initial unannealed sample contained 19 DOs out of a total of 192 Os. The hybrid MD/MC algorithm was run for 16 ps at 8000 K and produced a surface layer with only one single coordinated oxygen. The simulation was then continued for 30 ps using the variable temperature given by Eq. (6) with $\tau=2$ ps so that a $T_{\min}$ of 300 K was reached. Figure 4(b) clearly shows that there are no strong sites that might lead to hydrophilic behavior on a surface generated in this way.

IV. RESULTS AND DISCUSSION

There are several adsorption sites (AS) on the surface of Fig. 4(a) where the potential energy of a water molecule is more negative than the negative of heat of liquefaction of water at room temperature (−44 kJ/mol). In order to obtain a more detailed picture of these sites, their positions and energies were determined from the local minima of $U_{\min}(x,y)$ with respect to x and y in Fig. 4. Those minima $u_{\min}$ were arranged in ascending order. The five lowest are presented in Table I as the strongest absorption sites of Fig. 4(a). In addition, the strongest site of Fig. 4(b), which is hydrophobic by our definition, is also listed as site number 6 in the table.

To understand the reason for the strong water/surface interaction at the AS in Table I, we have decomposed the total energy $u_{\min}$ for a water molecule on an AS into its energies of interaction with separate tetrahedra u_i. Those energies were arranged in descending order of their absolute values. The six largest are presented in Table I. In what follows, we refer to the tetrahedron whose contribution to the energy of water on the jth AS is u_i as the ith tetrahedron of the jth AS so that, e.g., −152.4 in the first line of Table I is the energy of interaction of a water molecule on the first AS with the first tetrahedron. (The same tetrahedron may be referred to by different numbers if it makes contributions to different AS.)

It is seen from Table I that the major contribution to the adsorption energy of a water molecule on the strongest AS comes from its interaction with only one or two tetrahedra

TABLE I. Analysis of the strongest water adsorption sites. x and y-position of the site in Fig. 4. $u_{\min}$: Minimal potential energy of a water molecule at the site in kJ/mol. $u_1,\ldots,u_6$: The largest (in absolute value) contributions to $u_{\min}$ from separate SiO_4 tetrahedra.

No.	Fig.	x	y	$u_{\min}$	u_1	u_2	u_3	u_4	u_5	u_6
1	4(a)	−8.8	0.0	−94.7	−152.4	19.0	18.2	15.7	8.6	7.5
2	4(a)	−7.0	−8.8	−85.9	−120.9	11.5	10.5	9.1	5.9	−4.6
3	4(a)	−5.0	5.9	−56.2	−28.4	−26.7	4.2	−4.1	−3.6	3.4
4	4(a)	8.2	−5.9	−53.3	−27.8	−14.9	2.8	−2.4	−2.2	−2.1
5	4(a)	−5.9	3.2	−45.5	−33.2	−5.1	−2.9	−2.5	−1.9	−0.8
6	4(b)	−2.6	−6.4	−24.3	−14.0	−4.1	−3.5	3.5	−1.2	−1.0

out of a total of 120. To understand the reason for that, we decompose each u_i in Table I into contributions from point 2^l-pole moments ($l=0$: charge; $l=1$: dipole; $l=2$: quadrupole; etc.) of the ith tetrahedron with Si position at a distance r from the water molecule and a separate entry for the sum of the van der Waals energies of the water molecule interacting with O-atoms. (The van der Waals energy of a water with the Si cation is negligible compared to the O-water energies.) The calculated energies are presented as v_l ($l=0,\ldots,5$) and vdW in Table II. Each line in Table II corresponds to the ith tetrahedron of the jth AS where j is in the first column of Table II and i is the index of u_i on this line of Table II.

In calculating multipole moments of tetrahedra, the electric charges of O-atoms were divided by their coordinations as explained in Sec. III. (The same device was used to partition the dispersion/repulsion energies for Os belonging to more than one tetrahedron.) The values of quadrupole moments referred to below are the sums of the absolute values of their components.

Consider, for example, u_1 on the first line of Table I (the first tetrahedron of the first AS). The energy of interaction of this tetrahedron with a water molecule adsorbed on the first AS is 3.5 times more in absolute value than the heat of liquefaction of water. One may see from Table II that main contribution to this energy comes from electrostatic interactions. This tetrahedron contains a triply coordinated nonbridging oxygen so that its electric charge is positive. Its dipole and quadrupole moments are large which means that the tetrahedron is strongly distorted. Thus the major contribution to the adsorption energy of a water molecule on the first AS comes from a tetrahedron which contains DO and is strongly distorted. It is those defects that are responsible for the strong electrostatic interaction of a water molecule with this tetrahedron. A more detailed analysis is hampered by the fact that the distance between the water molecule and the center of multipole expansion is so short that the expansion either diverges or converges very slowly so that the electro-

TABLE II. Analysis of u_i ($i=1,2,3$) from the Table I. r is the distance from the Si-position in a tetrahedron to the O-position in the water molecule in Å. $l=0$, $l=1$, $l=2$: Sums of absolute values of components of 2^l-pole moments ($l=0,1,2,\ldots$: Charge, dipole, quadrupole, etc.; units of charge: Esu, units of length: Å.) of a tetrahedron. O-coord: Coordination with respect to Si of four O-atoms of a tetrahedron. v_l: Multipole components of u_i (v_3-v_5: Sum of $l=3$ to $l=5$ components). vdW: Van der Waals component of u_i.

No.	u_i	r	$l=0$	$l=1$	$l=2$	O-coord	v_0	v_1	v_2	v_3-v_5	vdW
	u_1	2.2	0.2	9.4	15.9	2 2 2 3	−25.2	−190.4	34.3	273.0	31.6
1	u_2	4.6	0.2	1.5	3.8	2 2 2 3	−4.9	2.8	1.1	7.2	12.3
	u_3	4.5	0	1.7	2.6	2 2 2 2	0	4.0	−1.8	7.3	8.6
	u_1	2.4	0.2	8.4	12.0	2 2 2 3	−20.5	−130.6	35.2	30.5	16.1
2	u_2	4.5	0	1.8	2.0	2 2 2 2	0	0.1	0	6.1	5.2
	u_3	4.7	0.2	1.5	2.9	2 2 2 3	−4.3	0.9	1.4	5.5	6.6
	u_1	4.0	0.2	8.4	12.0	2 2 2 3	−7.9	−25.0	12.8	−3.8	0.2
3	u_2	4.1	−0.6	2.6	7.8	1 2 2 2	−12.3	−8.8	−8.7	−5.0	6.4
	u_3	8.1	−0.6	4.1	6.6	1 2 2 2	4.4	−0.5	−0.2	0.4	−0.03
	u_1	4.1	−0.6	2.6	8.5	1 2 2 2	−12.4	−8.5	−10.3	−6.3	7.5
4	u_2	4.9	0.2	8.4	12.0	2 2 2 3	−5.1	−8.0	−5.2	2.7	−0.10
	u_3	8.0	−0.6	4.1	6.6	1 2 2 2	3.5	−0.6	0	0	−0.03
	u_1	4.4	−0.6	2.6	7.8	1 2 2 2	−14.2	−7.2	−9.0	−14.7	11.6
5	u_2	6.6	0.2	8.4	12.0	2 2 2 3	−1.6	−4.4	1.3	−0.2	−0.05
	u_3	10.2	−0.6	5.2	6.8	1 2 2 2	−3.0	−0.1	0.1	0.1	−0.01
	u_1	3.9	0	3.6	8.3	2 2 2 2	0	−4.2	−3.1	−8.5	1.2
6	u_2	4.0	0	1.6	11.2	2 2 2 2	0	−3.1	1.3	−4.3	1.8
	u_3	4.4	0	0.6	3.8	2 2 2 2	0	0.8	1.2	−6.0	0.12

static energy (u_1-vdW) does not equal the sum of v_l $l=0$ through $l=5$.

The other five largest contributions to $u_{\min}$ of the first AS in Table I are positive. This is the reason why $u_{\min}>u_1$. From Table II one may see that the main contribution to the interaction of the water molecule with the second and third tetrahedra of the first AS comes from their van der Waals repulsive energies. This means the O-atoms of those tetrahedra prevent the water molecule from taking the most favorable position and orientation where its electrostatic interactions with the first tetrahedron would have been even stronger.

The largest (in absolute value) contribution to the second AS in Tables I and II again comes from the tetrahedron closest to the water molecule with an energy 2.7 times more in absolute value than the heat of liquefaction of water and again, the four next largest contributions are repulsive. One feature is that now the first tetrahedron of the second AS is simultaneously the first tetrahedron of the third AS and the second tetrahedron of the fourth and fifth AS. This can be seen from the values of the dipole and quadrupole moments in Table II. The position of this tetrahedron (Si-position) in Fig. 4(a) is $x=-6.8$, $y=8.6$ which is close to the second AS. [Due to the PBC, the second AS is split into two parts in Fig. 4(a) at the upper and lower left corners.] This is also true for the first AS. One can see from Fig. 4(a) that second, third and fifth AS are close to each other. [The third AS is designated in the left upper corner of Fig. 4(a) by a closed contour.] Table II indicates that the second tetrahedron of the third AS is also the first tetrahedron of the fifth AS and the third tetrahedra of the third and fourth AS are, in fact, the same tetrahedron. Thus one tetrahedron can make considerable contributions to the adsorption energies of of water on several AS when they are close to each other.

For all the tetrahedra in Table II that are separated from a water molecule by a distance $r\geqslant 4$ Å, the multipole expansion of the electrostatic energy converges so that their interaction with the water molecule can be evaluated (to about 10%) by the sum of v_l $(l=0,...,5)$. The potential of a 2^l-pole decreases with distance as $1/r^{l+1}$ so that those tetrahedra which contain DO and are not electroneutral or are strongly distorted and therefore have large dipole moments can make considerable contribution to AS that are far away. In fact, all the tetrahedra in Table II corresponding to Fig. 4(a) contain DOs except the second tetrahedron of the second AS and the third tetrahedron of the first AS and, as explained above, the two tetrahedra that are almost regular make mainly repulsive contributions to the adsorption energy over the nearby AS.

Although we have shown that the surface corresponding to Fig. 4(a) contains strongly hydrophilic AS, one cannot be certain that the adsorption isotherm of water on this surface will be hydrophilic. Strictly speaking, it is not only the strength of separate AS that determines the hydrophilicity of a surface but also their concentration since hydrophilicity is a macroscopic, thermodynamic average property of a surface. To determine the degree of hydrophilicity of the surface of Fig. 4(a) one has to simulate the adsorption of water on that surface, which will be the next step of this work.

In contrast to the surface of Fig. 4(a), that of Fig. 4(b) is definitely hydrophobic since the binding energy of a water molecule on all its AS is less than the heat of liquefaction of water. Thus this surface certainly satisfies the criterion of hydrophobicity and thus may be considered as a possible model of a real amorphous silica surface. However, the atomic configuration corresponding to Fig. 4(b) is not an ideal random net as defined in Sec. I. Although it does not contain DOs, the distortion of tetrahedra, as seen from distribution of their dipole moments in Fig. 3, is greater than for the bulk. Thus the interaction of a water molecule on the strongest AS of Fig. 4(b) (last line of Table I) with the first tetrahedron (u_1) is -14 kJ/mol which is more negative than -11.6 kJ/mol, the minimum energy of interaction of a water molecule with a regular, nondistorted tetrahedron. The difference is not that large and it seems that the reason is, as shown in Table II, that the main contribution (-8.5 kJ/mol) to that interaction comes from higher multipole moments as for a regular tetrahedron. The main contribution to the binding energy of a water molecule on the strongest AS of Fig. 4(b) again comes from only one nearby tetrahedron. This might explain why the surface of real vitreous silica can be hydrophobic. It follows first of all from the value given above for the binding energy of a water molecule to a single undistorted tetrahedron is 1/4 the heat of liquefaction of water. Since it may be concluded from Table I that only one or two tetrahedra make major contributions to the total binding energy of a water molecule on the strongest AS, one may expect that the energy will not exceed the heat of liquefaction of water if the tetrahedra are nearly undistorted and the number of DOs is negligible. This, of course, is just a qualitative consideration; the quantitative evidence is given in Fig. 4(b).

Of course, the absolute values of the AS strengths in Fig. 4(b) depends on the parameters of the water–silica potential described in Sec. II. One can increase electrostatic interaction of a model water molecule with the surface just by increasing effective charges of the SPC model. However, to increase the absolute value of $u_{\min}$ on the last line of Table I to 44 kJ/mol, one has to increase those charges by the factor of 2 which seems rather unrealistic. Besides, if one increases those charges that much, the strengths of AS in Fig. 4(a) also increase beyond reasonable limits. In other words, the model surface corresponding to Fig. 4(b) is more realistic with respect to physical adsorption of water than that corresponding to Fig. 4(a), independent of the precise values of parameters of the water–silica interaction.

Another peculiarity of the surface corresponding to Fig. 4(b) is that it contains 2.6 edge-sharing tetrahedra per nm^2. Those edge-sharing tetrahedra may be considered as siloxane bridges that arise on the hydroxylated silica surface when two vicinal silanol groups condense into a water molecule and evaporate (see Sec. I). Since each siloxane bridge corresponds to two silanol groups, our totally dehydroxylated silica surface may be considered as a result of the dehydroxylation of a hydroxylated silica surface with 5.2 silanol groups per nm^2. The latter is the normal concentration of silanol groups on the surfaces of high surface area silicas.[35]

As mentioned in Sec. I, the ideal random network contains neither DO nor edge-sharing tetrahedra—both of them

should be considered as topological defects with respect to it. Thus although the method of simulation described in Sec. III eliminates DO from the surface, it increases the concentration of other topological defects (edge-sharing tetrahedra) with respect to previous simulations referred to in Sec. I. There is experimental evidence of the presence of edge-sharing tetrahedra at the surface of dehydroxylated vitreous silica. These were claimed to be the reason for two well-defined infrared bands at 888 and 907 cm^{-1} which arise after dehydroxylation of a high specific area silica.[36] However, the concentration of these edge-sharing tetrahedra was an order of magnitude smaller that that obtained in our simulation. There is a discussion of possible defect structures other than edge-shared tetrahedra in Ref. 36. It includes among others the paramagnetic, diamagnetic and double bonded NBOs. All of them were ruled out on the basis either of spectroscopic or chemical evidence. In particular, quantum chemical calculations show that an edge-shared tetrahedron is more stable than NBO.

V. CONCLUSION

We have shown that single or triple coordinated oxygen atoms as well as distorted SiO_4 tetrahedra at the surface of vitreous silica create a much stronger electrostatic field than that at a surface without these defects. This field interacts with water molecules and increases the hydrophilicity of the surface.

We have introduced a measure of tetrahedral distortion: the absolute values of their dipole and quadrupole moments. It is shown that these moments as well as uncompensated electrical charges on single and triple coordinated oxygen atoms plus higher multipole moments of distorted tetrahedra are responsible for strongly hydrophilic sites on the simulated surface of vitreous silica with concentrations of nonbridging oxygen atoms corresponding to previous simulations (see Sec. I). Those surfaces do not have the structures expected for hydrophobic behavior, in contradiction with the experimental finding that pure (not containing OH-groups) surfaces of high surface area silicas are hydrophobic.

By a special modification of molecular dynamics algorithm we have simulated a surface of vitreous silica that consists only of bridging oxygen atoms. This surface does not have hydrophilic sites, i.e., it is definitely hydrophobic.

Thus our results suggest that atomic structures of silica surfaces like dehydroxylated nonporous silica gels that are known to be hydrophobic contain single or triple coordinated oxygen atoms in much smaller concentrations than has been found in previous simulations (see Sec. I). It is very likely that the atomic structure of the silica surface depends strongly upon the process of its creation. A freshly fractured vitreous silica surface is expected to have a atomic structure other than that obtained by cooling the silica melt below the glass transition temperature. We do not know whether the freshly fractured surface of silica is hydrophobic or not. Discussion of this problem is, however, beyond the scope of this paper.

In a more general sense, our results show that computer simulation of physical adsorption of water (and other polar molecules as well) can be helpful in the characterization of the atomic structure of glass surfaces. This requires that one first simulate the surface, then simulate some adsorption characteristic on this surface and compare them with experimental data. This is a new direction in the study of glass surfaces. This paper is the first step in this direction but we do not believe that it solves the problem of the pure vitreous silica surface simulation. Hydrophobicity is a useful criterion that allows one to validate model atomic structures of vitreous silica surfaces but it does not mean that every simulated silica surface that passes such a test is an absolutely adequate model of the real silica surface.

While this paper was in the process of reviewing, we obtained additional arguments that its basic conclusions are valid. The vitreous silica surface was simulated by an independent method (a very slow and nonlinear annealing) and it was shown that it is composed only of bridging oxygens.[37] Adsorption of carbon dioxide was simulated on the surfaces described here as well as that of Ref. 37. The isotherms of adsorption on the hydrophobic surface described in this paper as well as that on the surface simulated in Ref. 37 are much closer to the experimental isotherm on nonporous silica than the isotherms simulated on surfaces with hydrophilic adsorption sites.[38]

ACKNOWLEDGMENT

This work was supported in part by the National Science Foundation through Grant No. DMR-9803884.

[1] P. H. Poole, P. F. McMillan, and G. H. Wolf, in *Structure, Dynamics and Properties of Silicate Melts*, edited by J. F. Stebbins, P. F. McMillan, and D. B. Dingwell [Rev. Mineral. **32**, 563–616 (1995)].
[2] S. H. Garofalini, J. Chem. Phys. **78**, 2069 (1983).
[3] S. M. Levine and S. H. Garofalini, J. Chem. Phys. **86**, 2997 (1987).
[4] B. P. Feuston and S. H. Garofalini, J. Chem. Phys. **91**, 564 (1989).
[5] A. E. Kohler, Jr. and S. H. Garofalini, Langmuir **10**, 4664 (1994).
[6] D. A. Litton and S. H. Garofalini, J. Non-Cryst. Solids **217**, 250 (1997).
[7] S. Blonski and S. H. Garofalini, J. Am. Ceram. Soc. **80**, 1997 (1997).
[8] G. Hochstrasser and J. F. Antonini, Surf. Sci. **32**, 644 (1972).
[9] C. G. Pantano, Rev. Solid State Sci. **3**, 379 (1989).
[10] D. Sprenger, H. Bach, W. Meisel, and P. Gütlich, J. Non-Cryst. Solids **126**, 111 (1990).
[11] H. Bach, J. Non-Cryst. Solids **209**, 1 (1997).
[12] J. Texter, K. Klier, and A. C. Zettlemoyer, Prog. Surf. Membrane Sci. **12**, 327 (1978); **12**, 339 (1978).
[13] S. J. Gregg and K. S. W. Sing, *Adsorption, Surface Area and Porosity*, (Academic, London, New York, 1982), pp. 269–274.
[14] V. Bolis, B. Fubini, L. Marchese, G. Martra, and D. Costa, J. Chem. Soc., Faraday Trans. **87**, 497 (1991).
[15] D. H. Olson, G. T. Kokotailo, S. L. Lawton, and W. M. Meier, J. Phys. Chem. **85**, 2238 (1981).
[16] S. Kondo, in *Adsorption on New and Modified Inorganic Sorbents*, edited by A. Dabrowski and V. A. Tertykh (Elsevier, New York, 1996), pp. 94 and 97.
[17] W. H. Zachariasen, J. Am. Chem. Soc. **54**, 3841 (1932).
[18] A. C. Wright, J. Non-Cryst. Solids **179**, 84 (1994).
[19] R. G. Della Valle and H. C. Andersen, J. Chem. Phys. **97**, 2682 (1992).
[20] B. P. Feuston and S. H. Garofalini, J. Appl. Phys. **68**, 4830 (1990).
[21] S. H. Garofalini, J. Non-Cryst. Solids **120**, 1 (1990).
[22] S. Tsuneyuki, M. Tsukada, H. Aoki, and Y. Matsui, Phys. Rev. Lett. **61**, 869 (1988).
[23] T. L. Gilbert, J. Chem. Phys. **49**, 2640 (1968).
[24] S. N. Taraskin and S. R. Elliott, Phys. Rev. B **56**, 8605 (1997).
[25] B. Guillot and Y. Guissani, Mol. Simul. **20**, 41 (1997).
[26] G. Boureau, S. Carniato, R. Tetot, and J. H. Harding, Mol. Simul. **20**, 27 (1997).

[27] E. S. Boek, P. V. Coveney, S. J. Williams, and A. S. Bains, Mol. Simul. **18**, 145 (1996).
[28] H. J. C. Berendsen, J. R. Grigera, and T. P. Straatsma, J. Phys. Chem. **91**, 6269 (1987).
[29] J. O. Hirschfelder, C. F. Curtiss, and R. B. Bird, *Molecular Theory of Gases and Liquids* (Wiley, New York, 1954), p. 1110.
[30] J. Horbach, W. Kob, K. Binder, and C. A. Angell, Phys. Rev. E **54**, R5897 (1996).
[31] Dann Frenkel and B. Smit, *Understanding Molecular Simulation* (Academic, New York, 1996).
[32] M. P. Allen and D. J. Tildesley, *Computer Simulation of Liquids* (Clarendon, New York, 1987).
[33] J. F. Stebbins, in *Structure, Dynamics and Properties of Silicate Melts*, edited by J. F. Stebbins, P. F. McMillan, and D. B. Dingwell [Rev. Mineral. **32**, 191 (1995)].
[34] W. H. Press, S. A. Teukolsky, W. T. Vetterling, and B. P. Flannery, *Numerical Recipes in FORTRAN* (Cambridge University, Cambridge, UK, 1992).
[35] L. T. Zhuravlev, Langmuir **3**, 316 (1987).
[36] B. C. Bunker, D. M. Maaland, K. J. Ward, T. A. Michalske, W. L. Smith, J. S. Binkley, C. F. Melius, and C. A. Balfe, Surf. Sci. **210**, 406 (1989).
[37] V. A. Bakaev, Phys. Rev. B (to be published).
[38] V. Bakaev, W. Steele, T. Bakaeva, and C. Pantano, J. Chem. Phys. **111**, 9813 (1999), following paper.